Shape Magnetic Anisotropy from Spin Density in Nanoscale Slab Systems

Tatsuki Oda[1,2,3], Indra Pardede[1], Tomosato Kanagawa[1], Nurul Ikhsan[1], Daiki Yoshikawa[1], and Masao Obata[1,2]
[1]Graduate School of Natural Science and Technology, Kanazawa University, Kakuma-machi, Kanazawa, 920- 1192, Japan
[2]Institute of Science and Engineering, Kanazawa University, Kakuma-machi, Kanazawa, 920-1192, Japan
[3]Center for Spintronics Research Network (CSRN), Osaka University, 1-3 Machikaneyama, Toyonaka, 560-8531, Japan

We developed a computational method for estimating magnetic dipole energy of slab materials using spin density obtained through a density functional approach. The new method can accurately estimate magnetic anisotropy energy for slabs from magnetic dipole interaction, called shape magnetic anisotropy energy (SMAE). We investigated ferromagnetic and antiferromagnetic slabs and found that a quadrupole component of atomic spin density suppresses SMAE in ferromagnetic slabs with Fe/MgO interface. In antiferromagnetic MnPt slabs, which have a perpendicular favor originating from the crystalline magnetic dipole interaction, a surface effect at the Mn edge appears as an enhancement of SMAE.

***Index Terms*—magnetic anisotropy energy, shape anisotropy, spin density functional theory, magnetic dipole interaction**

I. Introduction

THE magnetic anisotropy at the surface/interface plays an important role in magnetic properties of nanoscale size. The contribution of magnetic dipole-dipole coupling among electron spins cannot be neglected, as well as that of spin-orbit coupling in band electrons. Recently, complicated stackings of ferromagnetic materials or junctions between different kinds of magnets are focused in the materials for memory or sensor [1], [2], or for emerging new phenomena [3], [4], [5]. In this context, we developed a computational method for estimating magnetic anisotropy originating from the spin-orbit coupling in slabs [6]. To evaluate the total magnetic anisotropy in slabs more precisely, we propose a new computational method for magnetic dipole coupling [7]. To test the proposed method, we applied it to ferromagnetic slabs with multi-atomic monolayers and to antiferromagnetic slabs with perpendicular components from magnetic dipole coupling.

II. Computational method

A. Computational details

We carried out self-consistent calculations in order to obtain the data of magnetic moment densities $[\mathbf{m}(\mathbf{r})]$ and atomic magnetic moments in a spin density functional theory (SDFT) scheme [8], [9]. In this work, we investigated the shape magnetic anisotropy energy (SMAE) using the post-SDFT approaches; continuum approach (CA), discrete approach (DA), and spin density approach (SDA). The CA uses the data of total magnetization and a parameter of the slab thickness to evaluate the magnetic anisotropy energy (MAE) given by $\mathrm{MAE(CA)} = \mu_0 M^2/2\Omega$, where μ_0, M, and Ω are the vacuum permeability, total magnetic moment, and slab volume, respectively. In this formula, a uniform spin density is assumed in the magnetic slab. The DA uses the data of the atomic magnetic moments extracted from the spin density and evaluates the magnetic dipole energy given by the following formula in the Hartree unit [10],

$$E_{\mathrm{DA}} = \frac{1}{8c^2}{\sum_{\mathbf{R},\mathbf{t},\mathbf{t}'}}' \left[\frac{\mathbf{m_t}\cdot\mathbf{m_{t'}}}{|\mathbf{R}+\mathbf{t}-\mathbf{t}'|^3} - 3\frac{\{(\mathbf{R}+\mathbf{t}-\mathbf{t}')\cdot\mathbf{m_t}\}\{(\mathbf{R}+\mathbf{t}-\mathbf{t}')\cdot\mathbf{m_{t'}}\}}{|\mathbf{R}+\mathbf{t}-\mathbf{t}'|^5} \right], \quad (1)$$

where $c = 137.0370$, $\mathbf{R}$ indicates the translational lattice vector, $\mathbf{m_t}$ expresses the atomic magnetic moment integrated in a given atomic sphere with the spin density $\mathbf{m}(\mathbf{r})$, and the sum with the prime $\sum'$ indicates that the cases of $\mathbf{R}+\mathbf{t}-\mathbf{t}'=0$ are excluded. The SDA employs the following formula [11],

$$E_{\mathrm{SDA}} = \frac{1}{8c^2}\int\int d\mathbf{r}d\mathbf{r}' \left[\frac{\mathbf{m}(\mathbf{r})\cdot\mathbf{m}(\mathbf{r}')}{|\mathbf{r}-\mathbf{r}'|^3} - 3\frac{\{(\mathbf{r}-\mathbf{r}')\cdot\mathbf{m}(\mathbf{r})\}\{(\mathbf{r}-\mathbf{r}')\cdot\mathbf{m}(\mathbf{r}')\}}{|\mathbf{r}-\mathbf{r}'|^5} \right]. \quad (2)$$

The contribution to E_{SDA} at $\mathbf{r}=\mathbf{r}'$ should vanish due to the self-interaction of electrons, and the explicit treatment of the exclusion is usually necessary in a practical calculation. Comparing the DA and SDA, the intra-atomic contribution is not taken into account in the evaluation of E_{DA} except for the atomic moment, while E_{SDA} reflects the shape of the general spin density distribution. In the DA or SDA, the MAE is obtained as the energy difference between the magnetization alignments along perpendicular ([001]) and parallel ([100]) axes, such as $\mathrm{MAE(DA)} = E_{\mathrm{DA}}^{[001]} - E_{\mathrm{DA}}^{[100]}$ and $\mathrm{MAE(SDA)} = E_{\mathrm{SDA}}^{[001]} - E_{\mathrm{SDA}}^{[100]}$.

In the evaluation of E_{DA}, one can use an alternative method different from the previously used [10], [12]. In the SDA, replacing the real $\mathbf{m}(\mathbf{r})$ with the sum of Gaussian-shaped spherical atomic magnetic moment density (GSMM), E_{SDA} of (2) becomes equal to E_{DA}. The Gaussian shape was reconstructed with $m(\mathbf{r}) = \sum_I m_{a,I}\,\pi^{-3/2}\kappa^{-3}\exp(-|\mathbf{r}-\mathbf{R}_I|^2/\kappa^2)$, where κ is the Gaussian width and $m_{a,I}$ specifies the atomic magnetic moment on the I's atom. In this case, the Gaussian width should be reduced enough, for example

Manuscript received June 4, 2018; revised August 8, 2018 and August 24, 2018; accepted August 29, 2018. Corresponding author: T. Oda (email: oda@cphys.s.kanazawa-u.ac.jp).

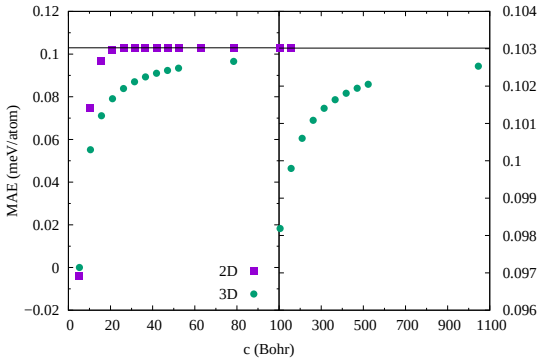

Fig. 1. Convergence of MAE with respect to c-axis for Fe square lattice slab using two-dimensional (squares) and three-dimensional (bullets) formula. a(lattice constant)=5.42 Bohr, $m_{\rm a} = 3\ \mu_{\rm B}$, and $\kappa = 1$ Bohr. Note that the horizontal and vertical scales are different between the left and the right panels.

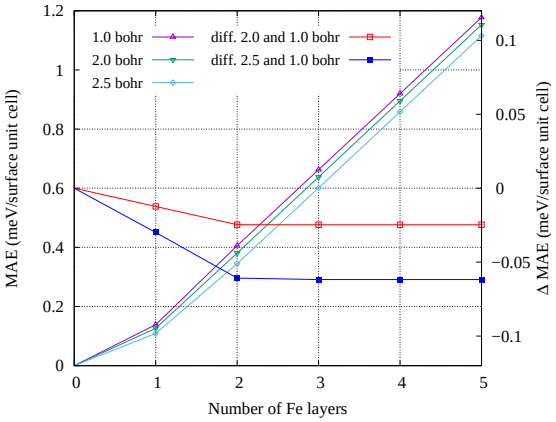

Fig. 2. Left axis: MAE(SDA) (plus, cross, asterisk) of free-standing Fe(xML) ($x = 1-5$) with GSMM density for Gaussian widths, $\kappa = 1, 2, 2.5$ Bohr. Right axis: square symbols indicate the difference from $\kappa = 1$ Bohr. The data on $x = 0$ is for the eye guide only.

$\kappa = 1$ Bohr ($= 0.0529$ nm), so that the neighboring atomic spin densities do not share the tails with each other.

In this work, we focus on slab systems and therefore need a formula particular to a two-dimensional version, as implied in [10]. Recently, an implementation of magnetic dipole energy has been developed in the SDFT code [7]. The implementation allows us to evaluate the magnetic dipole energy efficiently. In Fig. 1, a convergence of the magnetic dipole energy is shown with respect to c (cell dimension of c-axis) for a slab system (free-standing Fe atomic monolayer). The data of two-dimensional version converge rapidly, compared with those of three-dimensional one. Because in the evaluation the energy cut-offs of the plane wave basis for wave functions and electron densities are kept to fixed values (30 Ry and 300 Ry) [13], the larger c also corresponds to a higher accuracy.

III. Results and Discussion

A. Stacking effects in ferromagnetic slabs

In regard to the magnetic anisotropy of ferromagnetic layers, there are surface/interface effects and stacking effects. When the spin density distribution is distorted from a spherical shape on atomic magnetic density so that there is a quadrupole component in addition to the spherical, the MAE(SDA) varies from MAE(DA). A prolate (oblate) atomic magnetic density leads to a decrease (an increase) in the in-plane MAE [7]. Such effect may appear on the interface of metallic-ferromagnet/insulator as well as on the surface of the ferromagnetic slabs , as shown in this and next subsections.

When the atomic magnetic density shares the tails of the densities contributed from the neighboring atoms assuming spherical atomic density on each atom, the resulting MAE differs from the MAE(DA). Such effect may appear in metallic ferromagnetic slabs since the distance between the layers changes depending on the stacking sequence or interface circumstance. In Fig. 2, the MAE of free-standing Fe xML ($x = 1-5$) is shown for $E_{\rm SDA}$ with the GSMM density of the Gaussian width. In this evaluation, the Fe layer with a (001) surface was extracted from the BCC bulk Fe with the lattice constant of 5.42 Bohr, and $m_a = 3\ \mu_{\rm B}$. When κ (=1 Bohr) is small, the MAE changes linearly, showing no effect on the surface. In contrast, large κ (=2.5 Bohr) suppresses the in-plane MAE by 0.062 meV per surface unit cell (0.12 mJ/m^2) at the larger thicknesses ($x = 3, 4, 5$). This value indicates the surface effects on both sides of the slab, comparable to or larger than those of the experimental resolutions [1] or temperature effects [14].

Next, we investigated the MAE of MgO(5ML)/Fe(xML)/MgO(5ML) ($x = 1-10$) slab with the in-plane lattice constant extracted from MgO. This slab has vacuum layers of 0.9 nm thick on both sides of the layer. After the relaxation of layer distances, we estimated the MAEs for CA, DA, and SDA. The midpoint-to-midpoint layer distance between the Fe/MgO interfaces was taken as layer thickness. In order to identify the difference between the surface and interface effects, we also evaluated the MAE of an Fe(xML) slab obtained by deleting the MgO layers from the MgO/Fe(xML)/MgO slab. Our results are similar to the data of demagnetization energy in the previous work [15]. As shown in Fig. 3, the CA tends to provide larger values of MAEs ($E_{\rm CA}$), namely, a stronger in-plane anisotropy. In contrast, $E_{\rm SDA}$ is reduced by the surface/interface effect. This reduction is estimated by the difference between the intersections of linear fitting lines to be 0.163 mJ/m^2 and 0.166 mJ/m^2 for the slabs of MgO/Fe(xML)/MgO and Fe(xML), respectively. Similarity between these values tends to hide the difference between the interface effect of Fe/MgO and the surface effect of Fe-layer. When comparing the intersections of the DA and SDA, the corresponding differences are 0.109 mJ/m^2 and 0.073 mJ/m^2, indicating the difference between the interface and surface effects. The increasing rate of MAE with respect to the thickness, namely, the slope of linear fitting line in Fig. 3, does not vary with a large amount among the results of CA, DA, and SDA. This is due to the fact that the spin density distribution on the magnetic atom inside the layer (not at the interface/surface) has few quadrupole components.

Such quadrupole contribution is only observed in the interface layer. In Fig. 4(a), the radial spin density distributions of spherical and quadrupole components are shown for the

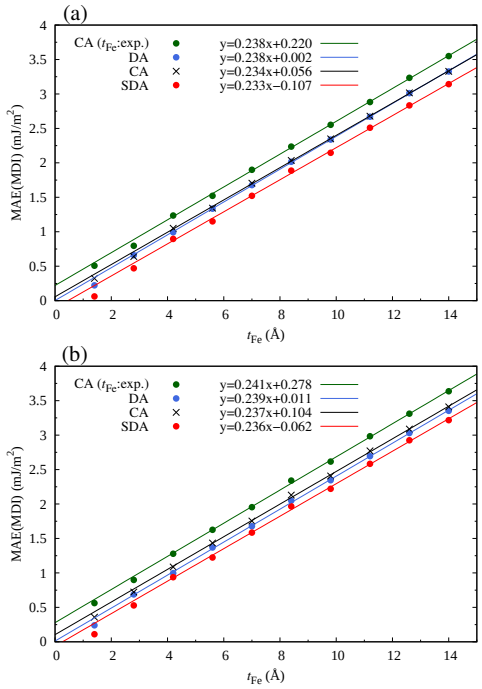

Fig. 3. MAEs of (a) MgO/Fe(xML)/MgO and (b) Fe(xML) ($x = 1 - 10$) for CA, DA, and SDA. The CA with the experimental thickness (0.14 nm/Fe ML) is also plotted. The lines are deduced from the least square fitting using the data of $x = 3 - 10$.

atoms on the interface and inside the layer. On the inside, the quadrupole component is reduced significantly compared with that on the interface. The origin of quadrupole spin density is based on the electron occupation of angular-dependent 3d orbitals. The prolate (oblate) type of atom-like spin density disfavors (favors) the in-plane shape anisotropy. Note that the surface effect discussed in Fig. 2 is negligible due to the fact that, as shown in Fig. 4, the spherical spin density distribution is damped enough outside the atomic region.

As shown in Fig. 3, the MAE of one or two Fe monolayer cases ($x = 1$ or 2) is suppressed from the value extrapolated from the data of thicker slabs. This is because the thinner slab has a part of surface/interface only. In such cases, extrapolation to a small thickness is no longer available, so the SDA is useful. In a ferromagnetic layer, such as Fe layer with an interface with MgO, the MAE originating from magnetic dipole interaction can be partially canceled out by a perpendicular MAE originating from the spin-orbit interaction [16]. The SDA is also useful for analyzing the MAE in slab systems. Recently, Ohno's group has investigated a thin film in which a magnetic alloy of $Fe_{75}B_{25}$ sandwiched with MgO [17] was used. The increasing rate of MAE with respect to the thickness seems to be lower than that in the present work. The difference in thickness and the FeB-alloying effect may provide a new starting point for future investigations on MAE.

B. Application in antiferromagnetic slabs

We investigated the MAE originating from the magnetic dipole interaction in a MnPt slab extracted from the bulk with $L1_0$ ordered alloy. Assuming an antiferromagnetic configuration is the same as in the bulk, where the total magnetization in the same Mn-atom layer vanishes and the atomic magnetic moments are parallel to those of the nearest-neighboring Mn layers, the DA and SDA were applied to several thicknesses (tML) with a (001) surface. The CA provides no contribution of MAE due to no magnetization. In the evaluations of $E_{\rm DA}$ and $E_{\rm SDA}$, a $\sqrt{2} \times \sqrt{2}$ magnetic unit cell was taken for an in-plane periodicity with the lattice constant of 7.56 Bohr.

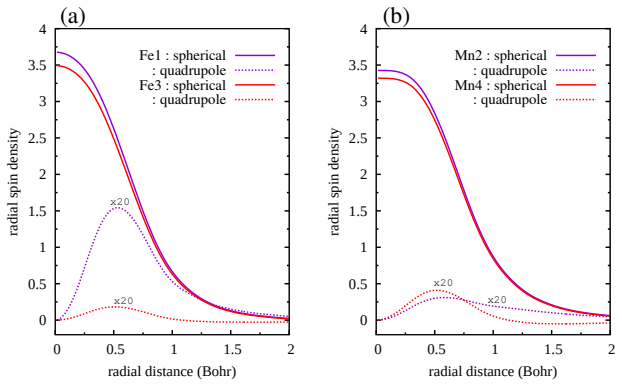

Fig. 4. Radial atomic spin density distribution [in (Bohr)$^{-3}$] in (a) MgO/Fe(5ML)/MgO and (b) MnPt(5ML). Fe1 and Mn2 indicate the interface/surface atoms, and Fe3 and Mn4 indicate the atoms inside the layer. All the quadrupole components are magnified 20 times.

As shown in Fig. 5, the negative signs of data indicate a perpendicular magnetic anisotropy. This perpendicular anisotropy is attributed to the antiferromagnetic spin alignment in each Mn atom-layer. The absolute of $E_{\rm SDA}$ is larger than that of $E_{\rm DA}$. Surface effects on the spin density distribution are clearly shown at the intersections of fitted linear lines between $E_{\rm DA}$ and $E_{\rm SDA}$. This is because the quadrupole component of atomic spin density distribution on the surface magnetic atom enhances the MAE. In Fig. 4(b), the typical quadrupole component on the surface Mn atom for MnPt(5ML) is shown. The difference in the intersection between $E_{\rm DA}$ and $E_{\rm SDA}$ is estimated to be 0.140 mJ/m^2 and 0.053 mJ/m^2 for the odd and even layers, respectively. The difference between these values is attributed to the difference of the surface edge termination. Both edges are Mn terminations in the odd layers and Mn and Pt terminations in the even layers.

The slope of the fitted linear line indicates a bulk-like property. The slopes of the odd and even layers are similar, resulting in the average of 0.094 mJ/m^2 per layer for the SDA. This perpendicular MAE is compiled to 0.094 meV/f.u. in a bulk form. The corresponding value of the DA is 0.087 meV/f.u. (0.087 mJ/m^2). The difference between the SDA and DA is 0.007 meV/f.u. This value is small but not negligible, originating from the quadrupole component on the Mn atom inside the layer (not on the surface). This is demonstrated in Fig. 4(b) where the quadrupole component inside the layer (Mn4 atom) is comparable to that on the surface (Mn2 atom). This may be caused by a tetragonal distortion in the bulk MnPt having the c/a ratio of 0.92 [18].

There is an in-plane MAE originating from the spin-orbit interaction of band electrons [19]. Cancellation between perpendicular and in-plane contributions is interesting to dis-

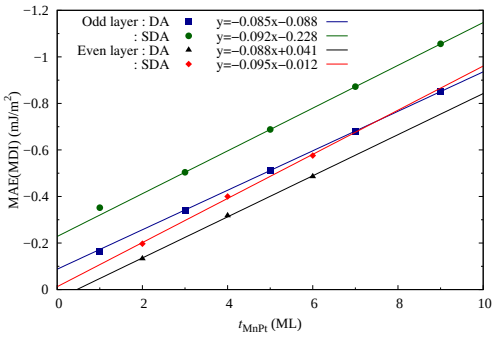

Fig. 5. MAE of the MnPt(tML) slab: Mn atomic monolayer ($t = 1$), $[\mathrm{MnPt}]_{(t-1)/2}$/Mn (odd layer), and $[\mathrm{MnPt}]_{t/2}$ (even layer). The data of $t = 1$ was not used for the linear fitting.

cuss. Considering the computational value (0.114 meV/f.u.) obtained with the SDFT approach by Lu *et al.* [19], the total MAE (0.02 meV/f.u.) indicates a relatively weak in-plane favor in magnetization. This value corresponds to 0.02 mJ/m^2 for a slab form. This smallness is consistent with the experimental ambiguity or observations of the transition from perpendicular to in-plane anisotropy under external perturbations [19]. Such kind of sensitivity of the total MAE allows us to design magnetic anisotropies. The computational design using the present scheme may also be combined with the spin-orbit interaction.

IV. Conclusion

We investigated the SMAE of the ferromagnetic MgO/Fe(xML)/MgO slab and antiferromagnetic MnPt(tML) slab using the CA, DA, and SDA. The recently developed SDA allowed us to estimate the SMAE more accurately based on the realistic spin density obtained in the first-principles approach. The SDA is able to include the effect of non-spherical spin density distribution, such as quadrupole atomic spin density. Such spin density distribution at the interface/surface or bulk-like site showed non-negligible variations of the MAE. This new approach using spin density may be useful for analyzing a subtle balance between different anisotropy origins, for example, origins of in-plane and out-of-plane.

Acknowledgment

This work was supported in part by the Scientic Research from JSPS/MEXT under Grants 15K05165 and 18K04923, in part by the ImPACT Program of Council for Science, Technology, and Innovation (Cabinet Ofce, Japan Government), in part by the Computational Materials Science Initiative, Japan, and in part by the Advanced Institute for Computational Science and Information Technology Center of Nagoya University through the High Performance Computing Infrastructure (HPCI) System Research Project under Project hp160227 and Project hp160107. N. Ikhsan and I. Pardede would like to thank the Japanese Government (MEXT) for the Scholarship in the Program for the Development of Global Human Resources at Kanazawa University. The first-principles calculations were performed using the facilities of the Supercomputer Center, Institute for Solid State Physics, University of Tokyo, Japan.

References

[1] T. Nozaki, A. Kozio-Rachwa, W. Skowroski, V. Zayets, Y. Shiota, S. Tamaru, H. Kubota, A. Fukushima, S. Yuasa, and Y. Suzuki, "Large Voltage-Induced Changes in the Perpendicular Magnetic Anisotropy of an MgO-Based Tunnel Junction with an Ultrathin Fe Layer," *Phys. Rev. Appl.*, vol. 5, pp. 044006, 2016.

[2] M. Gottwald, S. Andrieu, F. Gimbert, E. Shipton, L. Calmels, Csar Magn, E. Snoeck, M. Liberati, T. Hauet, E. Arenholz, Stphane Mangin, and E. E. Fullerton, "Co/Ni (111) superlattices studied by microscopy, x-ray absorption, and ab initio calculations," *Phys. Rev. B*, vol. 86, pp. 014425, 2012.

[3] S. Fukami, C. Zhang, S. DuttaGupta, A. Kurenkov, and H. Ohno, "Magnetization switching by spin-orbit torque in an antiferromagnet/ferromagnet bilayer system," *Nat. Mat.*, vol. 15, pp. 535541, 2016.

[4] T. Nozaki, Y. Shiokawa, Y. Kitaoka, Y. Kota, H. Imamura, M. Al-Mahdawi, S. P. Pati, S. Ye, S. Yonemura, T. Shibata, and M. Sahashi, "Large perpendicular exchange bias and high blocking temperature in Al-doped Cr_2O_3/Co thin film systems," *Appl. Phys. Express*, vol. 10, pp. 073003, 2017.

[5] T. Jungwirth, X. Marti, P. Wadley, and J. Wunderlich, "Antiferromagnetic spintronics," *Nat. Nanotech.*, vol. 11, pp. 231241, 2016.

[6] M. Tsujikawa, A. Hosokawa and T. Oda, "Magnetic Anisotropy of Fe/Pt(001) and Pt/Fe/Pt(001) Using a First-Principles Approach," *Phys. Rev. B*, vol. 77, pp. 054413(1-10), 2008.

[7] T. Oda and M. Obata, "Implementation of magnetic dipole interaction in the planewave-basis approach for slab systems," *J. Phys. Soc. Jpn.*, vol. 87, no. 6, pp. 064803, 2018.

[8] U. von Barth and L. Hedin, "A local exchange-correlation potential for the spin polarized case: I" *J. Phys. C: Solid State Phys.*, vol. 5, pp. 1629, 1972.

[9] J. P. Perdew, J. A. Chevary, S. H. Vosko, K. A. Jackson, M. R. Pederson, D. J. Singh, and C. Fiolhais, "Atoms, molecules, solids, and surfaces: Applications of the generalized gradient approximation for exchange and correlation," *Phys. Rev. B*, vol. 46, pp. 6671, 1992.

[10] L. Szunyogh, B. Újfalussy, and P. Weinberger, "Magnetic anisotropy of iron multilayers on Au(001): First-principles calculations in terms of the fully relativistic spin-polarized screened KKR method," *Phys. Rev. B*, vol. 51, pp. 9552, 1995.

[11] G. H. O. Daalderop, P. J. Kelly, M. F. H. Schuurmans, and F. Jansen, "First-principles calculation of the magnetocrystalline anisotropy energy of iron, cobalt, and nickel," *Phys. Rev. B*, vol. 41, pp. 11919, 1990.

[12] H. J. G. Draaisma and W. J. M. de Jonge, "Surface and volume anisotropy from dipole- dipole interactions in ultrathin ferromagnetic films," *J. Appl. Phys.*, vol. 64, pp. 3610, 1988.

[13] K. Laasonen, A. Pasquarello, R. Car, C. Lee, and D. Vanderbilt, "Car-Parrinello molecular dynamics with Vanderbilt ultrasoft pseudopotentials," *Phys. Rev. B*, vol. 47, pp. 10142, 1993.

[14] Q. Xiang, Z. Wen, H. Sukegawa, S. Kasai, T. Seki, T. Kubota, K. Takanashi and S. Mitani, "Nonlinear electric field effect on perpendicular magnetic anisotropy in Fe/MgO interfaces," *J. Phys. D: Appl. Phys.*, vol. 50, pp. 40LT04, 2017.

[15] A. Hallal, H. X. Yang, B. Dieny, and M. Chshiev, "Anatomy of perpendicular magnetic anisotropy in Fe/MgO magnetic tunnel junctions: First principles insight," *Phys. Rev. B*, vol. 88, no. 18, pp. 184423, 2013.

[16] R. Shimabukuro, K. Nakamura, T. Akiyama, and T. Ito, "Electric field effects on magnetocrystalline anisotropy in ferromagnetic Fe monolayers," *Physica E*, vol. 42, no. 4, pp. 1014-1017, 2010.

[17] K. Watanabe, B. Jinnai, S. Fukami, H. Sato, and H. Ohno, "Shape anisotropy revisited in single-digit nanometer magnetic tunnel junctions," *Nat. Commun.*, vol. 9, pp. 663 (1-6), 2018.

[18] P. Ravindran, A. Kjekshus, H. Fjellvåg, P. James, L. Nordström, B. Johansson, O. Eriksson, "Large magnetocrystalline anisotropy in bilayer transition metal phases from first-principles full-potential calculations," *Phys. Rev. B*, vol. 63, no. 14, pp. 144409, 2001.

[19] Z. Lu, R. V. Chepulskii, and W. H. Butler, "First-principles study of magnetic properties of $L1_0$-ordered MnPt and FePt alloys," *Phys. Rev. B*, vol. 81, no. 9, pp. 094437, 2010.